Z boson pair-production at LEP

P. Achard, O. Adriani, M. Aguilar-Benitez, J. Alcaraz, G. Alemanni, J. Allaby, A. Aloisio, M.G. Alviggi, H. Anderhub, V.P. Andreev, et al.

EUROPEAN ORGANIZATION FOR NUCLEAR RESEARCH

CERN-EP/2003-034
June 20, 2003

Z Boson Pair-Production at LEP

The L3 Collaboration

Abstract

Events stemming from the pair-production of Z bosons in e^+e^- collisions are studied using $217.4\,pb^{-1}$ of data collected with the L3 detector at centre-of-mass energies from 200 GeV up to 209 GeV. The special case of events with b quarks is also investigated.

Combining these events with those collected at lower centre-of-mass energies, the Standard Model predictions for the production mechanism are verified. In addition, limits are set on anomalous couplings of neutral gauge bosons and on effects of extra space dimensions.

Submitted to *Phys. Lett. B*

1 Introduction

The pair-production of Z bosons in e^+e^- collisions at LEP was observed [1] with the L3 detector [2] once the accelerator centre-of-mass energy, $\sqrt{s}$, exceeded the production threshold of $2m_Z$, where m_Z denotes the Z boson mass. Numerous studies from data samples collected at the steadily increasing $\sqrt{s}$ and integrated luminosities were reported by L3 [3, 4] and other collaborations [5].

In the Standard Model of the electroweak interactions [6], the Z pair-production is described at the lowest order by two t-channel Feynman diagrams with an internal electron[1)] leg, collectively denoted as NC02. A wider definition is used in this Letter: all diagrams leading to two fermion-antifermion pairs are considered and kinematic restrictions which enhance the NC02 contribution are enforced. Results in the NC02 framework are also given.

The study of Z pair-production offers a further test of the Standard Model in the neutral gauge boson sector and is of particular relevance as this process constitutes an irreducible background in the search for the Standard Model Higgs boson at LEP. Events with Z boson decaying into b quarks have a signature similar to those originated by the process $e^+e^- \to ZH \to f\bar{f}b\bar{b}$. Their selection and the measurement of their cross section validate the experimental procedures used in the search of the Standard Model Higgs boson.

Z pair-production allows the investigation of the anomalous triple neutral gauge boson couplings ZZZ and ZZγ [7], forbidden at tree level in the Standard Model and tests new theories like possible effects of extra space dimensions [8].

This Letter describes measurements at two average values of $\sqrt{s}$, 204.8 GeV and 206.6 GeV, corresponding to integrated luminosities of $78.5\,\mathrm{pb}^{-1}$ and $138.9\,\mathrm{pb}^{-1}$, respectively. Hereafter, these data samples are denoted as the 205 GeV and 207 GeV energy bins. Combined results from the full Z pair-production sample collected with the L3 detector are also given in the comparison with Standard Model expectations and for constraints on New Physics.

2 Monte Carlo simulations

The EXCALIBUR [9] Monte Carlo program is used to model signal and background neutral-current four-fermion processes. The Z pair-production process is defined as the subset of the four-fermion generated phase space satisfying the following kinematics cuts [1, 3, 4]. The invariant mass of fermion-antifermion pairs is required to be between 70 GeV and 105 GeV. For events with two identical pairs, at least one of the possible pairings has to satisfy this condition. For the $u\bar{d}d\bar{u}$, $c\bar{s}s\bar{c}$ and $\nu_\ell\ell^+\bar{\nu}_\ell\ell^-$ ($\ell = e, \mu, \tau$) final states, the masses of the pairs that could originate from a W decay have to be either below 75 GeV or above 85 GeV. The polar angle θ_e of generated electrons is required to satisfy $|\cos\theta_e| < 0.95$.

The Z pair-production cross section is calculated to be 1.07 pb and 1.08 pb for the 205 GeV and 207 GeV energy bins, respectively. Following a comparison with the GRC4F [10] Monte Carlo generator, and taking into account the modelling of initial state radiation, an uncertainty of 2% is assigned to these calculations.

The cross section for final states with b quark pairs is significantly smaller. Combining the two energy bins a cross-section of 0.30 pb, also with an uncertainty of 2%, is expected for an average centre-of-mass energy $\sqrt{s} = 205.9$ GeV.

[1)] In this Letter, the word electron is used for both electrons and positrons.

Four-fermion events generated with EXCALIBUR which do not satisfy the signal definition are considered as background. Background from fermion pair-production is described by KK2f [11] for the processes $e^+e^- \to q\overline{q}(\gamma)$, $e^+e^- \to \mu^+\mu^-(\gamma)$ and $e^+e^- \to \tau^+\tau^-(\gamma)$, and BHWIDE [12] for $e^+e^- \to e^+e^-(\gamma)$. Background from charged-current four-fermion processes is generated with EXCALIBUR for the $e\nu_e q\bar{q}'$ final state and with KORALW [13] for W pair-production and decay in final states not covered by the simulations listed above. Hadron and lepton production in two-photon processes is modelled by PHOJET [14] and DIAG36 [15], respectively.

The L3 detector response is simulated using the GEANT program [16], which takes into account the effects of energy loss, multiple scattering and showering in the detector. GHEISHA [17] is used for the simulation of hadronic interactions. Time dependent detector inefficiencies, as monitored during the data taking period, are also reproduced.

3 Event selection

All visible final states of Z pair-production are investigated. For the $q\bar{q}\nu\bar{\nu}$, $\ell^+\ell^-\nu\bar{\nu}$ and $\ell^+\ell^-\ell'^+\ell'^-$ final states, criteria are used which are similar to those developed at $\sqrt{s} = 189$ GeV [3] and $\sqrt{s} = 192 - 202$ GeV [4]. For the $q\bar{q}q'\bar{q}'$ and $q\bar{q}\ell^+\ell^-$ final states, improved analyses are devised. All selections rely on the identification of two fermion pairs with masses close to m_Z.

Electrons are identified by requiring a well isolated electromagnetic cluster in the electromagnetic calorimeter with an associated track in the tracking chamber. To increase efficiency, the track matching requirement is relaxed in some selections.

Muons are reconstructed from the coincidence of tracks in the muon spectrometer and the central tracker which are in time with the beam crossing. Energy depositions in the calorimeters which are compatible with a minimum ionising particle (MIP) and have an associated track in the central tracker are also accepted.

Taus are identified by their decays either into electrons or muons, or into hadrons detected as narrow and isolated low multiplicity jets associated with one, two or three tracks.

Quark fragmentation and hadronisation yields a high multiplicity of calorimetric clusters and charged tracks. These are grouped into jets by means of the DURHAM algorithm [18]. The number of reconstructed jets depends on the thresholds y_{mn} for which a m-jet event is reconstructed as a n-jet one.

The tagging of b quarks [19] relies on the reconstruction of the decay vertices of weakly decaying b-hadrons with the silicon vertex detector and the central tracker. The shape and particle content of the associated jets are also considered.

The four-momenta of neutrinos are derived from all other particles measured in the event, making use of the hermeticity of the detector.

3.1 The $q\bar{q}q'\bar{q}'$ channel

The study of the $q\bar{q}q'\bar{q}'$ channel [20] starts by selecting high multiplicity events with a visible energy, E_{vis}, satisfying $0.75 < E_{vis}/\sqrt{s} < 1.35$. The energy imbalance in the directions parallel and perpendicular to the beam axis have to be less than $0.2E_{vis}$ and $0.25E_{vis}$, respectively. These criteria suppress fermion-pair production, two-photon interactions and four-fermion final states with leptons. To further reduce boson pair-production with leptons, events with isolated electrons or muons with an energy larger than 40 GeV are rejected. Events with isolated photons of energies above 25 GeV are also rejected.

The remaining events are forced into four jets. A kinematic fit which imposes four-momentum conservation is performed to improve the di-jet mass resolution. Among the three possible jet pairings, the pairing i is chosen which minimizes:

$$\chi^2_{\mathrm{ZZ}} = \left(\Sigma_i - 2m_{\mathrm{Z}}\right)^2 / \sigma^2_{\Sigma_{\mathrm{ZZ}}} + \Delta_i^2 / \sigma^2_{\Delta_{\mathrm{ZZ}}},$$

where Σ_i and Δ_i are the di-jet mass sum and differences and $\sigma^2_{\Sigma_{\mathrm{ZZ}}}$ and $\sigma^2_{\Delta_{\mathrm{ZZ}}}$ their resolutions, determined from Monte Carlo. Only events for which $\Sigma_i > 165$ GeV are retained.

The remaining background is formed by events from the $\mathrm{e^+e^-} \to \mathrm{W^+W^-}$ and $\mathrm{e^+e^-} \to \mathrm{q\bar{q}}(\gamma)$ processes. A likelihood, L^{Sel}_{ZZ}, is built which combines ten variables: the event sphericity, the largest triple jet boost [21], the largest jet energy and boost, the largest energy difference between any two jets, the opening angle between the most and least energetic jets, $\log y_{34}$, the mass M_{5C} from a kinematic fit with equal mass constraint, the absolute value of the cosine of the polar angle of the event thrust vector, $|\cos\theta_T|$, χ^2_{ZZ} and the corresponding variable for the W-pair hypothesis, χ^2_{WW}. The distributions of L^{Sel}_{ZZ} for data and Monte Carlo are shown in Figure 1. Events with $L^{Sel}_{\mathrm{ZZ}} < 0.1$ are mostly due to the $\mathrm{e^+e^-} \to \mathrm{q\bar{q}}(\gamma)$ process and are not considered in the following.

A second likelihood, L_{ZZ}, is built to further exploit the difference between Z pair-production and the residual background from W pair-production. It uses seven variables: L^{Sel}_{ZZ}, Σ_{ZZ}, the corresponding variable for the W-pair hypothesis, Σ_{WW}, the three to four-jet threshold for the JADE clustering algorithm [22], the event thrust and the value of the b-tag variable for the two jets with the highest probability to originate from b quarks.

The distributions of L_{ZZ} for data and Monte Carlo are shown in Figure 2a. Table 1 lists the yield of this selection for $L_{\mathrm{ZZ}} > 0.2$, which corresponds to an efficiency of 55.4%.

3.2 The $\mathrm{q\bar{q}}\nu\bar{\nu}$ channel

The selection of the $\mathrm{q\bar{q}}\nu\bar{\nu}$ channel is identical to that performed at $\sqrt{s} = 192 - 202$ GeV [4]. High multiplicity events with large missing energy and momentum and no high energy isolated electrons, muons or photons are selected. They are forced into two jets and a constrained fit which enforces the hypothesis that the missing four-momentum is due to a Z boson is applied.

Finally, an artificial neural network singles out Z pair-production events from background. Its input variables include event shape variables that differentiate a two-jet from a three-jet topology, the sum of visible and missing masses, the masses of the two jets, the missing momentum and the energy in a 25° azimuthal sector around the missing momentum vector.

Figure 2b shows the output of the neural network, NN_{out}, for data and Monte Carlo. The results of this selection are summarised in Table 1 for a benchmark cut $NN_{out} > 0.5$, which corresponds to an efficiency of 46.2%.

3.3 The $\mathrm{q\bar{q}}\ell^+\ell^-$ channel

The study of the $\mathrm{q\bar{q}e^+e^-}$, $\mathrm{q\bar{q}}\mu^+\mu^-$ and $\mathrm{q\bar{q}}\tau^+\tau^-$ final states [23] proceeds from a sample of high multiplicity events, well balanced in the planes parallel and transverse to the beam direction. Background from two-photon interactions is rejected by requiring $|\cos\theta_T| < 0.98$. Events from the $\mathrm{e^+e^-} \to \mathrm{q\bar{q}}(\gamma)$ process with hard initial state radiation photons are reduced by requiring the effective centre-of-mass energy [24], $\sqrt{s'}$, to be greater than $0.55\sqrt{s}$. Remaining two-jet events are suppressed by a cut on the event thrust.

To fully reconstruct the $q\bar{q}\ell^+\ell^-$ final state, after identifying an electron, muon or tau pair in the event, the remaining clusters are forced into two jets. A kinematic fit which enforces energy and momentum conservation and equal mass, M_{5C}, of the hadronic and leptonic systems is performed. To cope with different background contributions, different selection criteria are applied for the three final states.

The $q\bar{q}e^+e^-$ selection requires low transverse energy imbalance and a sum of the energies of the two electrons close to $\sqrt{s}/2$. The variable $(E_1 + E_2 - E_3 - E_4)/(E_1 + E_2 + E_3 + E_4)$, is also considered, where E_i denotes the decreasingly ordered jet and lepton energies. This variable has low values for the signal, where the energy is uniformly distributed among the four particles, and large values for the background from the $e^+e^- \to q\bar{q}(\gamma)$ process. An efficiency of 73.9% is reached.

The $q\bar{q}\mu^+\mu^-$ final state has a low background contamination, almost entirely rejected by requiring a large energy for the lowest energetic muon, expected to be soft for background events. This selection has an efficiency of 60.4%.

The $q\bar{q}\tau^+\tau^-$ selection is affected by a larger background. It requires the invariant mass of the hadronic system prior to the kinematic fit to be compatible with m_Z and a large rest frame angle between the taus. In addition, the sum of the di-jet and di-tau masses after the kinematic fit has to be close to $2m_Z$. This selection accepts 28.0% of the $q\bar{q}\tau^+\tau^-$ final states, as well as 2.4% and 4.8% of the $q\bar{q}e^+e^-$ and $q\bar{q}\mu^+\mu^-$ final states, respectively.

Table 1 presents the combined yield of all selections, whose overall efficiency is 55.4%. Figure 2c shows the M_{5C} distributions for data and Monte Carlo.

3.4 The $\ell^+\ell^-\nu\bar{\nu}$ channel

Only final states with electrons and muons are considered with a selection identical to that performed at lower $\sqrt{s}$ [4]. A pair of acoplanar leptons is selected in low multiplicity events with large missing momentum pointing away from the beam axis. To improve efficiency, electrons are not required to have an associated track. To reduce the background, no MIP candidates are accepted in the muon selection. Both the lepton visible mass, $M_{\ell\ell}$, and recoil mass, M_{rec}, must be consistent with m_Z. These criteria suppress background from fermion pair-production. Residual background from four-fermion processes is reduced by performing a fit which constrains the leptons to originate from a Z boson and requiring the recoil mass to be close to m_Z.

For signal events, the sum $M_{\ell\ell} + M_{rec}$ should be close to $2m_Z$. The distributions of this variable for data and Monte Carlo, combined with results from the $\ell^+\ell^-\ell'^+\ell'^-$ channel, are shown in Figure 2d. An efficiency of 25.3% is achieved and the results of the selection are reported in Table 1.

3.5 The $\ell^+\ell^-\ell'^+\ell'^-$ channel

The selection for the $\ell^+\ell^-\ell'^+\ell'^-$ channel aims to retain a high efficiency to compensate for the low branching ratio. The same criteria of Reference 4 are applied to select low multiplicity events with four or more loosely identified leptons, with energy above 3 GeV. Events must contain at least one electron or muon pair. Electrons without an associated track are accepted while MIPs are not considered to form these pairs.

The lepton pair with mass closest to m_Z is selected and both $M_{\ell\ell}$ and M_{rec} are required to be compatible with m_Z. Background from fermion pair-production is reduced by imposing upper bounds on the opening angle of the leptons of this pair.

The sum $M_{\ell\ell} + M_{rec}$ is used as a final discriminating variable. Its data and Monte Carlo distributions are presented in Figure 2d, together with those from the $\ell^+\ell^-\nu\bar{\nu}$ channel. The yield of the selection is summarized in Table 1 and corresponds to an efficiency of 33.6%.

4 Results

4.1 Measurement of the ZZ cross section

The cross sections for each energy bin and each final state are derived [4] with a fit to the final discriminating variables and are presented in Table 1 together with the Standard Model predictions. In the presence of fluctuations for channels with low statistics, an upper limit [4] on the cross section is given. Fixing the relative contributions of all channels to the Standard Model expectations, the Z pair-production cross section is extracted and also presented in Table 1. All the measured cross-sections agree with their Standard Model predictions.

4.2 Study of systematic uncertainties

Several sources of systematic uncertainty are considered [4] and listed in Table 2. Systematic effects correlated among channels arise from uncertainties on the detector energy scales, on the signal modelling, as derived from a comparison between EXCALIBUR and GRC4F and on the prediction of the background level. This is studied by varying the expected cross sections for W pair-production, jet production, the $e\nu_e q\bar{q}'$ and four-fermion processes by 0.5%, 5%, 10% and 5%, respectively. The $q\bar{q}q'\bar{q}'$ channel is affected by uncertainties on the charge multiplicity and the simulation of the b-tag discriminant. Other sources of systematic uncertainty, uncorrelated among the channels, are the signal and background Monte Carlo statistics, detailed in Table 3 and the accuracy of the simulation of the selection variables and of those used for the lepton identification.

Including all systematic uncertainties, the measured cross sections read:[2)]

$$\begin{aligned}
\sigma_{ZZ}(205\,\mathrm{GeV}) &= 0.78 \pm 0.20\,(\mathrm{stat.}) \pm 0.05\,(\mathrm{syst.}) \quad (\mathrm{SM}: 1.07 \pm 0.02\,\mathrm{pb}) \\
\sigma_{ZZ}(207\,\mathrm{GeV}) &= 1.10 \pm 0.17\,(\mathrm{stat.}) \pm 0.07\,(\mathrm{syst.}) \quad (\mathrm{SM}: 1.08 \pm 0.02\,\mathrm{pb}),
\end{aligned}$$

Figure 3 presents these values together with lower energy measurements [1, 3, 4].

4.3 Final states with b quarks

The final discriminant of the $q\bar{q}q'\bar{q}'$ analysis, plotted in Figure 2a, shows a high sensitivity to final states containing b quarks. In order to tag $b\bar{b}\nu\bar{\nu}$ and $b\bar{b}\ell^+\ell^-$ final states, the b-tag information of the two jets are combined [4] to form the discriminating variables shown in Figure 4. For the $b\bar{b}\nu\bar{\nu}$ final state, the value of the variable NN_{out} is also considered in the combination. The cross sections for Z pair-production with b quarks in the final states are

[2)] In the NC02 framework, the cross sections are derived as:

$$\begin{aligned}
\sigma_{ZZ}^{NC02}(205\,\mathrm{GeV}) &= 0.77 \pm 0.20\,(\mathrm{stat.}) \pm 0.05\,(\mathrm{syst.}) \quad (\mathrm{SM}: 1.05 \pm 0.02\,\mathrm{pb}) \\
\sigma_{ZZ}^{NC02}(207\,\mathrm{GeV}) &= 1.09 \pm 0.17\,(\mathrm{stat.}) \pm 0.07\,(\mathrm{syst.}) \quad (\mathrm{SM}: 1.07 \pm 0.02\,\mathrm{pb}),
\end{aligned}$$

where the Standard Model expectations, consistent among the EXCALIBUR, ZZTO [25] and YFSZZ [26] programs, are assigned an uncertainty of 2%.

determined from a fit to these variables and listed in Table 4. Their combination gives a total cross section:

$$\sigma_{\mathrm{ZZ}\to\mathrm{b\bar{b}X}}\,(205 - 207\ \mathrm{GeV}) = 0.24 \pm 0.09\,(\mathrm{stat}) \pm 0.03\,(\mathrm{sys}).$$

The systematic uncertainty follows from the sources discussed above and is detailed in Table 2.

4.4 Combined results

The ratio between measured and expected cross sections, $R_{\mathrm{ZZ}} = \sigma^{fit}/\sigma^{th}$, is calculated including lower energy data [1, 3, 4] as:

$$R_{\mathrm{ZZ}}\,(183 - 209\ \mathrm{GeV}) \quad = \quad 0.93 \pm 0.08\,(\mathrm{stat}) \pm 0.06\,(\mathrm{sys}).$$

Systematic uncertainties include correlations among different data samples. The predictions are in agreement with the measurements with a precision of 11%.

Figure 5a shows the distribution of the reconstructed mass M_{Z} of the Z boson, and Figure 5b the absolute value of the cosine of the observed production angle θ_{Z} for the full Z pair-production sample. The cuts $L_{\mathrm{ZZ}} > 0.85$ and $NN_{out} > 0.8$ are applied to data decsribed in this Letter. Data at lower energies [1, 3, 4] are also included.

5 Limits on physics beyond the Standard Model

5.1 Anomalous couplings

Assuming on-shell production of the two Z bosons, anomalous ZZV couplings are parametrised [7] by the coefficients f_i^{V}, with $i = 4, 5$ and $\mathrm{V} = \gamma, \mathrm{Z}$. The f_4^{V} coefficients correspond to CP violation and the f_5^{V} ones to CP conservation. All f_i^{V} coefficients are zero in the Standard Model. Each event of the signal Monte Carlo distributions presented in Figure 2 is reweighted [3] to simulate anomalous values of the f_i^{V} coefficients. The full phase space of the Z boson pair, as reconstructed from the jet and lepton four-momenta, is used. A fit to these distribution is performed leaving one coupling free at a time and fixing the others to zero, yielding the 95% confidence level limits:

$$-0.48 \le f_4^{\mathrm{Z}} \le 0.46; \quad -0.36 \le f_5^{\mathrm{Z}} \le 1.03; \quad -0.28 \le f_4^{\gamma} \le 0.28; \quad -0.40 \le f_5^{\gamma} \le 0.47,$$

compatible with the Standard Model expectations. Lower energy data [1, 3, 4] are included in the fit. Figure 6 presents results of simultaneous fits to couplings with the same CP eigenvalue.

5.2 Extra space dimensions

A recent theory [27], dubbed "Low Scale Gravity", proposes a solution to the hierarchy problem by postulating a scale M_S for the gravitational interactions which is of the order of the electroweak scale. Extra space dimensions are a consequence of this theory. In this scenario, spin-two gravitons contribute to the Z pair-production [8], interfering with the Standard Model production mechanism. The Z pair-production cross sections presented in this Letter and those measured at lower energies [1,3,4] are fit with a combination of Low Scale Gravity and Standard Model contributions. A lower 95% confidence level limit on the scale M_S of 0.7 TeV is obtained. It holds for both constructive and destructive interference between the Low Scale Gravity and the Standard Model contributions.

References

[1] L3 Collab., M. Acciarri *et al.*, Phys. Lett. **B 450** (1999) 281.

[2] L3 Collab., B. Adeva *et al.*, Nucl. Inst. Meth. **A 289** (1990) 35; L3 Collab., O. Adriani *et al.*, Phys. Rept. **236** (1993) 1; I. C. Brock *et al.*, Nucl. Instr. and Meth. **A 381** (1996) 236; M. Chemarin *et al.*, Nucl. Inst. Meth. **A 349** (1994) 345; M. Acciarri *et al.*, Nucl. Inst. Meth. **A 351** (1994) 300; A. Adam *et al.*, Nucl. Inst. Meth. **A 383** (1996) 342; G. Basti *et al.*, Nucl. Inst. Meth. **A 374** (1996) 293.

[3] L3 Collab., M. Acciarri *et al.*, Phys. Lett. **B 465** (1999) 363.

[4] L3 Collab., M. Acciarri *et al.*, Phys. Lett. **B 497** (2001) 23.

[5] ALEPH Collab., R. Barate *et al.*, Phys. Lett. **B 469** (1999) 287; DELPHI Collab., P. Abreu *et al.*, Phys. Lett. **B 497** (2001) 199; DELPHI Collab., J. Abdallah *et al.*, Preprint CERN-EP/2003-009 (2003); OPAL Collab., G. Abbiendi *et al.*, Phys. Lett. **B 476** (2000) 256.

[6] S.L. Glashow, Nucl. Phys. **22** (1961) 579; A. Salam, in Elementary Particle Theory, ed. N. Svartholm, (Almqvist and Wiksell, Stockholm, 1968), p. 367; S. Weinberg, Phys. Rev. Lett. **19** (1967) 1264; M. Veltman, Nucl. Phys. **B 7** (1968) 637; G.M. 't Hooft, Nucl. Phys. **B 35** (1971) 167; G.M. 't Hooft and M. Veltman, Nucl. Phys. **B 44** (1972) 189; G.M. 't Hooft and M. Veltman, Nucl. Phys. **B 50** (1972) 318.

[7] K. Hagiwara *et al.*, Nucl. Phys. **B 282** (1987) 253; J. Alcaraz *et al.*, Phys. Rev. **D 61** (2000) 075006; G. J. Gounaris, J. Layssac and F. M. Renard, Phys. Rev. **D 61** (2000) 073013.

[8] K. Agashe and N. G. Deshpande, Phys. Lett. **B 456** (1999) 60; L3 Collab., M. Acciarri *et al.*, Phys. Lett. **B 464** (1998) 135; L3 Collab., M. Acciarri *et al.*, Phys. Lett. **B 470** (1999) 281; S. Mele and E. Sanchez, Phys. Rev. **D 61** (2000) 117901.

[9] R. Kleiss and R. Pittau, Comp. Phys. Comm. **85** (1995) 437.

[10] J. Fujimoto *et al.*, Comp. Phys. Comm. **100** (1997) 128.

[11] S. Jadach, B.F.L. Ward and Z. Wąs, Comp. Phys. Comm. **130** (2000) 260.

[12] S. Jadach *et al.*, Phys. Lett. **B 390** (1997) 298.

[13] M. Skrzypek *et al.*, Comp. Phys. Comm. **94** (1996) 216; M. Skrzypek *et al.*, Phys. Lett. **B 372** (1996) 289.

[14] R. Engel, Z. Phys. **C 66** (1995) 203; R. Engel and J. Ranft, Phys. Rev. **D 54** (1996) 4244.

[15] F.A. Berends, P.H. Daverfelt and R. Kleiss, Nucl. Phys. **B 253** (1985) 441; Comp. Phys. Comm. **40** (1986) 285.

[16] The L3 detector simulation is based on GEANT Version 3.15. R. Brun *et al.*, "GEANT 3", CERN–DD/EE/84–1 (Revised), 1987.

[17] H. Fesefeldt, RWTH Aachen Report PITHA **85/02** (1985).

[18] S. Bethke *et al.*, Nucl. Phys. **B 370** (1992) 310.

[19] David Aaron Matzner Dominguez, Search for Neutral Higgs Bosons in e^+e^- Interactions at center-of-mass energies between 130 GeV and 183 GeV, Ph.D. thesis, University of California, San Diego, 1998.

[20] Serge Likhoded, Search for the Higgs Boson and a Study of $e^+e^- \to ZZ$ Using the L3 Detector at LEP, Ph.D. thesis, Humboldt University, Berlin, 2002.

[21] L3 Collab., P. Achard *et al.*, Phys. Lett. **B 517** (2001) 319.

[22] JADE Collab., W. Bartel *et al.,* Z. Phys. **C 33** (1986) 23; JADE Collab., S. Bethke *et al.,* Phys. Lett. **B 213** (1988) 235.

[23] Gagan Mohanty, Study of Z-Boson Pair Production and Search for Physics beyond Standard Model at LEP-II, Ph.D. thesis, University of Mumbai, 2002.

[24] L3 Collab., M. Acciarri *et al.*, Phys. Lett. **B 479** (2000) 101.

[25] M.W. Grünewald *et al.*, Preprint hep-ph/0005309 (2000).

[26] S. Jadach, B.F.L. Ward and Z. Wąs, Phys. Rev. **D 56** (1997) 6939.

[27] N. Arkani-Hamed *et al.*, Phys. Lett. **B 429** (1998) 263.

The L3 Collaboration:

P.Achard,[20] O.Adriani,[17] M.Aguilar-Benitez,[24] J.Alcaraz,[24] G.Alemanni,[22] J.Allaby,[18] A.Aloisio,[28] M.G.Alviggi,[28] H.Anderhub,[46] V.P.Andreev,[6,33] F.Anselmo,[8] A.Arefiev,[27] T.Azemoon,[3] T.Aziz,[9] P.Bagnaia,[38] A.Bajo,[24] G.Baksay,[25] L.Baksay,[25] S.V.Baldew,[2] S.Banerjee,[9] Sw.Banerjee,[4] A.Barczyk,[46,44] R.Barillère,[18] P.Bartalini,[22] M.Basile,[8] N.Batalova,[43] R.Battiston,[32] A.Bay,[22] F.Becattini,[17] U.Becker,[13] F.Behner,[46] L.Bellucci,[17] R.Berbeco,[3] J.Berdugo,[24] P.Berges,[13] B.Bertucci,[32] B.L.Betev,[46] M.Biasini,[32] M.Biglietti,[28] A.Biland,[46] J.J.Blaising,[4] S.C.Blyth,[34] G.J.Bobbink,[2] A.Böhm,[1] L.Boldizsar,[12] B.Borgia,[38] S.Bottai,[17] D.Bourilkov,[46] M.Bourquin,[20] S.Braccini,[20] J.G.Branson,[40] F.Brochu,[4] J.D.Burger,[13] W.J.Burger,[32] X.D.Cai,[13] M.Capell,[13] G.Cara Romeo,[8] G.Carlino,[28] A.Cartacci,[17] J.Casaus,[24] F.Cavallari,[38] N.Cavallo,[35] C.Cecchi,[32] M.Cerrada,[24] M.Chamizo,[20] Y.H.Chang,[48] M.Chemarin,[23] A.Chen,[48] G.Chen,[7] G.M.Chen,[7] H.F.Chen,[21] H.S.Chen,[7] G.Chiefari,[28] L.Cifarelli,[39] F.Cindolo,[8] I.Clare,[13] R.Clare,[37] G.Coignet,[4] N.Colino,[24] S.Costantini,[38] B.de la Cruz,[24] S.Cucciarelli,[32] J.A.van Dalen,[30] R.de Asmundis,[28] P.Déglon,[20] J.Debreczeni,[12] A.Degré,[4] K.Dehmelt,[25] K.Deiters,[44] D.della Volpe,[28] E.Delmeire,[20] P.Denes,[36] F.DeNotaristefani,[38] A.De Salvo,[46] M.Diemoz,[38] M.Dierckxsens,[2] C.Dionisi,[38] M.Dittmar,[46] A.Doria,[28] M.T.Dova,[10,♯] D.Duchesneau,[4] M.Duda,[1] B.Echenard,[20] A.Eline,[18] A.El Hage,[1] H.El Mamouni,[23] A.Engler,[34] F.J.Eppling,[13] P.Extermann,[20] M.A.Falagan,[24] S.Falciano,[38] A.Favara,[31] J.Fay,[23] O.Fedin,[33] M.Felcini,[46] T.Ferguson,[34] H.Fesefeldt,[1] E.Fiandrini,[32] J.H.Field,[20] F.Filthaut,[30] P.H.Fisher,[13] W.Fisher,[36] I.Fisk,[40] G.Forconi,[13] K.Freudenreich,[46] C.Furetta,[26] Yu.Galaktionov,[27,13] S.N.Ganguli,[9] P.Garcia-Abia,[24] M.Gataullin,[31] S.Gentile,[38] S.Giagu,[38] Z.F.Gong,[21] G.Grenier,[23] O.Grimm,[46] M.W.Gruenewald,[16] M.Guida,[39] R.van Gulik,[2] V.K.Gupta,[36] A.Gurtu,[9] L.J.Gutay,[43] D.Haas,[5] D.Hatzifotiadou,[8] T.Hebbeker,[1] A.Hervé,[18] J.Hirschfelder,[34] H.Hofer,[46] M.Hohlmann,[25] G.Holzner,[46] S.R.Hou,[48] Y.Hu,[30] B.N.Jin,[7] L.W.Jones,[3] P.de Jong,[2] I.Josa-Mutuberría,[24] D.Käfer,[1] M.Kaur,[14] M.N.Kienzle-Focacci,[20] J.K.Kim,[42] J.Kirkby,[18] W.Kittel,[30] A.Klimentov,[13,27] A.C.König,[30] M.Kopal,[43] V.Koutsenko,[13,27] M.Kräber,[46] R.W.Kraemer,[34] A.Krüger,[45] A.Kunin,[13] P.Ladron de Guevara,[24] I.Laktineh,[23] G.Landi,[17] M.Lebeau,[18] A.Lebedev,[13] P.Lebrun,[23] P.Lecomte,[46] P.Lecoq,[18] P.Le Coultre,[46] J.M.Le Goff,[18] R.Leiste,[45] M.Levtchenko,[26] P.Levtchenko,[33] C.Li,[21] S.Likhoded,[45] C.H.Lin,[48] W.T.Lin,[48] F.L.Linde,[2] L.Lista,[28] Z.A.Liu,[7] W.Lohmann,[45] E.Longo,[38] Y.S.Lu,[7] C.Luci,[38] L.Luminari,[38] W.Lustermann,[46] W.G.Ma,[21] L.Malgeri,[20] A.Malinin,[27] C.Maña,[24] J.Mans,[36] J.P.Martin,[23] F.Marzano,[38] K.Mazumdar,[9] R.R.McNeil,[6] S.Mele,[18,28] L.Merola,[28] M.Meschini,[17] W.J.Metzger,[30] A.Mihul,[11] H.Milcent,[18] G.Mirabelli,[38] J.Mnich,[1] G.B.Mohanty,[9] G.S.Muanza,[23] A.J.M.Muijs,[2] B.Musicar,[40] M.Musy,[38] S.Nagy,[15] S.Natale,[20] M.Napolitano,[28] F.Nessi-Tedaldi,[46] H.Newman,[31] A.Nisati,[38] T.Novak,[30] H.Nowak,[45] R.Ofierzynski,[46] G.Organtini,[38] I.Pal,[43] C.Palomares,[24] P.Paolucci,[28] R.Paramatti,[38] G.Passaleva,[17] S.Patricelli,[28] T.Paul,[10] M.Pauluzzi,[32] C.Paus,[13] F.Pauss,[46] M.Pedace,[38] S.Pensotti,[26] D.Perret-Gallix,[4] B.Petersen,[30] D.Piccolo,[28] F.Pierella,[8] M.Pioppi,[32] P.A.Piroué,[36] E.Pistolesi,[26] V.Plyaskin,[27] M.Pohl,[20] V.Pojidaev,[17] J.Pothier,[18] D.Prokofiev,[33] J.Quartieri,[39] G.Rahal-Callot,[46] M.A.Rahaman,[9] P.Raics,[15] N.Raja,[9] R.Ramelli,[46] P.G.Rancoita,[26] R.Ranieri,[17] A.Raspereza,[45] P.Razis,[29] D.Ren,[46] M.Rescigno,[38] S.Reucroft,[10] S.Riemann,[45] K.Riles,[3] B.P.Roe,[3] L.Romero,[24] A.Rosca,[45] S.Rosier-Lees,[4] S.Roth,[1] C.Rosenbleck,[1] B.Roux,[30] J.A.Rubio,[18] G.Ruggiero,[17] H.Rykaczewski,[46] A.Sakharov,[46] S.Saremi,[6] S.Sarkar,[38] J.Salicio,[18] E.Sanchez,[24] C.Schäfer,[18] V.Schegelsky,[33] H.Schopper,[47] D.J.Schotanus,[30] C.Sciacca,[28] L.Servoli,[32] S.Shevchenko,[31] N.Shivarov,[41] V.Shoutko,[13] E.Shumilov,[27] A.Shvorob,[31] D.Son,[42] C.Souga,[23] P.Spillantini,[17] M.Steuer,[13] D.P.Stickland,[36] B.Stoyanov,[41] A.Straessner,[18] K.Sudhakar,[9] G.Sultanov,[41] L.Z.Sun,[21] S.Sushkov,[1] H.Suter,[46] J.D.Swain,[10] Z.Szillasi,[25,¶] X.W.Tang,[7] P.Tarjan,[15] L.Tauscher,[5] L.Taylor,[10] B.Tellili,[23] D.Teyssier,[23] C.Timmermans,[30] Samuel C.C.Ting,[13] S.M.Ting,[13] S.C.Tonwar,[9] J.Tóth,[12] C.Tully,[36] K.L.Tung,[7] J.Ulbricht,[46] E.Valente,[38] R.T.Van de Walle,[30] R.Vasquez,[43] V.Veszpremi,[25] G.Vesztergombi,[12] I.Vetlitsky,[27] D.Vicinanza,[39] G.Viertel,[46] S.Villa,[37] M.Vivargent,[4] S.Vlachos,[5] I.Vodopianov,[25] H.Vogel,[34] H.Vogt,[45] I.Vorobiev,[34,27] A.A.Vorobyov,[33] M.Wadhwa,[5] Q.Wang,[30] X.L.Wang,[21] Z.M.Wang,[21] M.Weber,[1] P.Wienemann,[1] H.Wilkens,[30] S.Wynhoff,[36] L.Xia,[31] Z.Z.Xu,[21] J.Yamamoto,[3] B.Z.Yang,[21] C.G.Yang,[7] H.J.Yang,[3] M.Yang,[7] S.C.Yeh,[49] An.Zalite,[33] Yu.Zalite,[33] Z.P.Zhang,[21] J.Zhao,[21] G.Y.Zhu,[7] R.Y.Zhu,[31] H.L.Zhuang,[7] A.Zichichi,[8,18,19] B.Zimmermann,[46] M.Zöller.[1]

1 III. Physikalisches Institut, RWTH, D-52056 Aachen, Germany[§]
2 National Institute for High Energy Physics, NIKHEF, and University of Amsterdam, NL-1009 DB Amsterdam, The Netherlands
3 University of Michigan, Ann Arbor, MI 48109, USA
4 Laboratoire d'Annecy-le-Vieux de Physique des Particules, LAPP,IN2P3-CNRS, BP 110, F-74941 Annecy-le-Vieux CEDEX, France
5 Institute of Physics, University of Basel, CH-4056 Basel, Switzerland
6 Louisiana State University, Baton Rouge, LA 70803, USA
7 Institute of High Energy Physics, IHEP, 100039 Beijing, China[△]
8 University of Bologna and INFN-Sezione di Bologna, I-40126 Bologna, Italy
9 Tata Institute of Fundamental Research, Mumbai (Bombay) 400 005, India
10 Northeastern University, Boston, MA 02115, USA
11 Institute of Atomic Physics and University of Bucharest, R-76900 Bucharest, Romania
12 Central Research Institute for Physics of the Hungarian Academy of Sciences, H-1525 Budapest 114, Hungary[‡]
13 Massachusetts Institute of Technology, Cambridge, MA 02139, USA
14 Panjab University, Chandigarh 160 014, India.
15 KLTE-ATOMKI, H-4010 Debrecen, Hungary[¶]
16 Department of Experimental Physics, University College Dublin, Belfield, Dublin 4, Ireland
17 INFN Sezione di Firenze and University of Florence, I-50125 Florence, Italy
18 European Laboratory for Particle Physics, CERN, CH-1211 Geneva 23, Switzerland
19 World Laboratory, FBLJA Project, CH-1211 Geneva 23, Switzerland
20 University of Geneva, CH-1211 Geneva 4, Switzerland
21 Chinese University of Science and Technology, USTC, Hefei, Anhui 230 029, China[△]
22 University of Lausanne, CH-1015 Lausanne, Switzerland
23 Institut de Physique Nucléaire de Lyon, IN2P3-CNRS,Université Claude Bernard, F-69622 Villeurbanne, France
24 Centro de Investigaciones Energéticas, Medioambientales y Tecnológicas, CIEMAT, E-28040 Madrid, Spain[♭]
25 Florida Institute of Technology, Melbourne, FL 32901, USA
26 INFN-Sezione di Milano, I-20133 Milan, Italy
27 Institute of Theoretical and Experimental Physics, ITEP, Moscow, Russia
28 INFN-Sezione di Napoli and University of Naples, I-80125 Naples, Italy
29 Department of Physics, University of Cyprus, Nicosia, Cyprus
30 University of Nijmegen and NIKHEF, NL-6525 ED Nijmegen, The Netherlands
31 California Institute of Technology, Pasadena, CA 91125, USA
32 INFN-Sezione di Perugia and Università Degli Studi di Perugia, I-06100 Perugia, Italy
33 Nuclear Physics Institute, St. Petersburg, Russia
34 Carnegie Mellon University, Pittsburgh, PA 15213, USA
35 INFN-Sezione di Napoli and University of Potenza, I-85100 Potenza, Italy
36 Princeton University, Princeton, NJ 08544, USA
37 University of Californa, Riverside, CA 92521, USA
38 INFN-Sezione di Roma and University of Rome, "La Sapienza", I-00185 Rome, Italy
39 University and INFN, Salerno, I-84100 Salerno, Italy
40 University of California, San Diego, CA 92093, USA
41 Bulgarian Academy of Sciences, Central Lab. of Mechatronics and Instrumentation, BU-1113 Sofia, Bulgaria
42 The Center for High Energy Physics, Kyungpook National University, 702-701 Taegu, Republic of Korea
43 Purdue University, West Lafayette, IN 47907, USA
44 Paul Scherrer Institut, PSI, CH-5232 Villigen, Switzerland
45 DESY, D-15738 Zeuthen, Germany
46 Eidgenössische Technische Hochschule, ETH Zürich, CH-8093 Zürich, Switzerland
47 University of Hamburg, D-22761 Hamburg, Germany
48 National Central University, Chung-Li, Taiwan, China
49 Department of Physics, National Tsing Hua University, Taiwan, China
§ Supported by the German Bundesministerium für Bildung, Wissenschaft, Forschung und Technologie
‡ Supported by the Hungarian OTKA fund under contract numbers T019181, F023259 and T037350.
¶ Also supported by the Hungarian OTKA fund under contract number T026178.
♭ Supported also by the Comisión Interministerial de Ciencia y Tecnología.
♯ Also supported by CONICET and Universidad Nacional de La Plata, CC 67, 1900 La Plata, Argentina.
△ Supported by the National Natural Science Foundation of China.

Channel	$\sqrt{s}$ (GeV)	N_D	N_S	N_B	σ^{fit} (pb)	σ^{th} (pb)
$q\bar{q}q'\bar{q}'$	205	166	24.9 ± 0.0	140.5 ± 0.4	$0.38^{+0.20}_{-0.17}$	0.51
	207	300	46.6 ± 0.0	255.1 ± 0.6	$0.55^{+0.15}_{-0.14}$	0.52
$q\bar{q}\nu\bar{\nu}$	205	13	10.8 ± 0.1	11.0 ± 0.1	< 0.24	0.30
	207	36	19.3 ± 0.1	18.7 ± 0.1	$0.25^{+0.08}_{-0.08}$	0.30
$q\bar{q}\ell^+\ell^-$	205	10	6.8 ± 0.1	1.6 ± 0.1	$0.19^{+0.08}_{-0.06}$	0.16
	207	18	12.3 ± 0.0	3.0 ± 0.1	$0.19^{+0.06}_{-0.05}$	0.16
$\ell^+\ell^-\nu\bar{\nu}$	205	2	0.9 ± 0.0	0.6 ± 0.0	$0.08^{+0.09}_{-0.06}$	0.04
	207	3	1.6 ± 0.1	1.2 ± 0.0	$0.05^{+0.06}_{-0.04}$	0.04
$\ell^+\ell^-\ell'^+\ell'^-$	205	0	0.4 ± 0.0	0.2 ± 0.0	< 0.11	0.02
	207	1	0.7 ± 0.0	0.4 ± 0.0	$0.08^{+0.09}_{-0.06}$	0.02
$e^+e^- \to ZZ$	205	191	43.8 ± 0.1	154.0 ± 0.4	0.78 ± 0.20	1.07
	207	358	80.4 ± 0.1	278.4 ± 0.6	1.10 ± 0.17	1.08

Table 1: Number of observed data events, N_D and signal, N_S, and background, N_B, expected Monte Carlo events in the two energy bins. The benchmark criteria $L_{ZZ} > 0.2$ and $NN_{Out} > 0.5$ are applied for the $q\bar{q}q'\bar{q}'$ and $q\bar{q}\nu\bar{\nu}$ final states, respectively. Uncertainties are due to Monte Carlo statistics. Measured, σ^{fit}, and expected, σ^{th}, cross sections are also given. Limits on σ^{fit} are at the 95% confidence level.

	$\delta\sigma_{ZZ}$ (%)	$\delta\sigma_{ZZ\to b\bar{b}X}$ (%)
Correlated sources		
Energy scale	3.1	2.4
Theory predictions	2.0	2.0
WW cross section	0.4	0.5
Four-jet rate	1.4	2.7
Weν cross section	1.1	0.8
Four-fermion cross section	0.5	0.5
Uncorrelated sources		
Charge multiplicity	1.3	2.3
B-tag	2.5	11.3
Monte Carlo statistics	1.9	3.1
Simulation	3.5	3.5
Total	6.4	13.2

Table 2: Systematic uncertainties on σ_{ZZ} and $\sigma_{ZZ\to b\bar{b}X}$.

	$q\bar{q}\ell^+\ell^-$	$q\bar{q}\nu\bar{\nu}$	$q\bar{q}q'\bar{q}'$	$\ell^+\ell^-\nu\bar{\nu}$	$\ell^+\ell^-\ell'^+\ell'^-$
Signal MC statistics (σ_{ZZ})	0.5 %	0.4 %	<0.1 %	3.0 %	1.0 %
Background MC statistics (σ_{ZZ})	3.4 %	0.5 %	0.2 %	0.1 %	0.2 %
Signal MC statistics ($\sigma_{ZZ\to b\bar{b}X}$)	3.9 %	1.8 %	2.1 %	–	–
Background MC statistics ($\sigma_{ZZ\to b\bar{b}X}$)	3.4 %	1.4 %	2.2 %	–	–
Simulation	4.8 %	3.2 %	1.6 %	0.8 %	1.8 %

Table 3: Sources of uncorrelated systematic uncertainties on σ_{ZZ} and $\sigma_{ZZ\to b\bar{b}X}$.

	$b\bar{b}\ell^+\ell^-$	$b\bar{b}\nu\bar{\nu}$	$q\bar{q}b\bar{b}$
Measured cross section (pb)	0.032 ± 0.027	< 0.108	0.185 ± 0.074
Expected cross section (pb)	0.035	0.065	0.201

Table 4: Cross sections for final states with b quarks. The limit is at 95% confidence level.

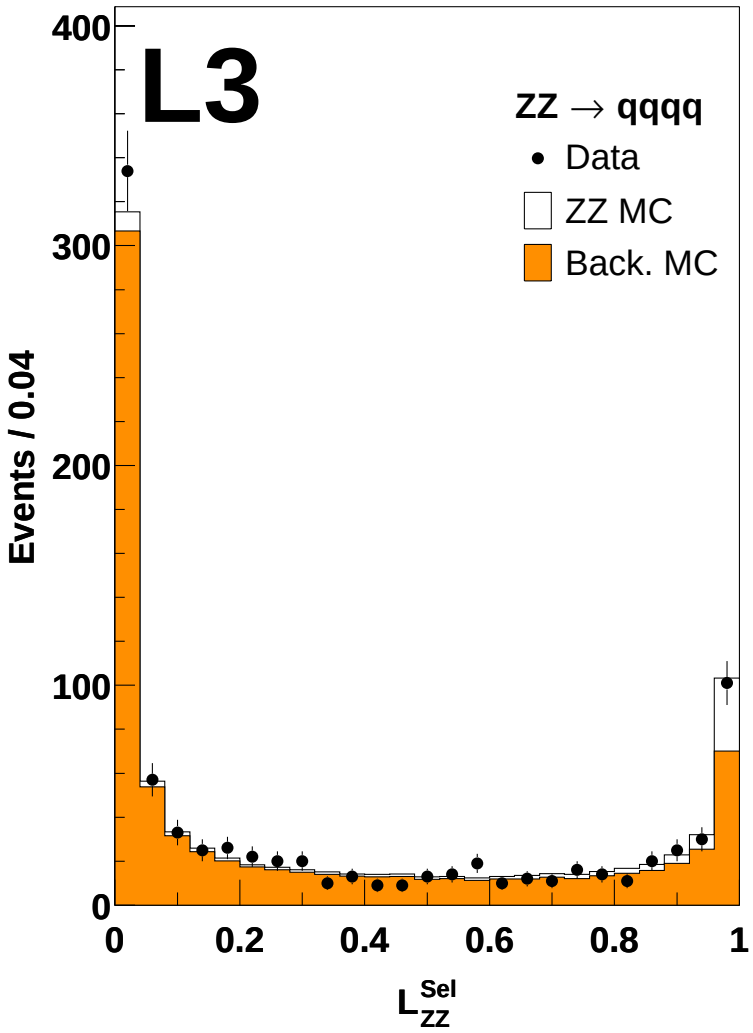

Figure 1: Distribution of the likelihood L_{ZZ}^{Sel} used for the $q\bar{q}q'\bar{q}'$ selection. The signal and background Monte Carlo distributions are normalised to the expected cross sections.

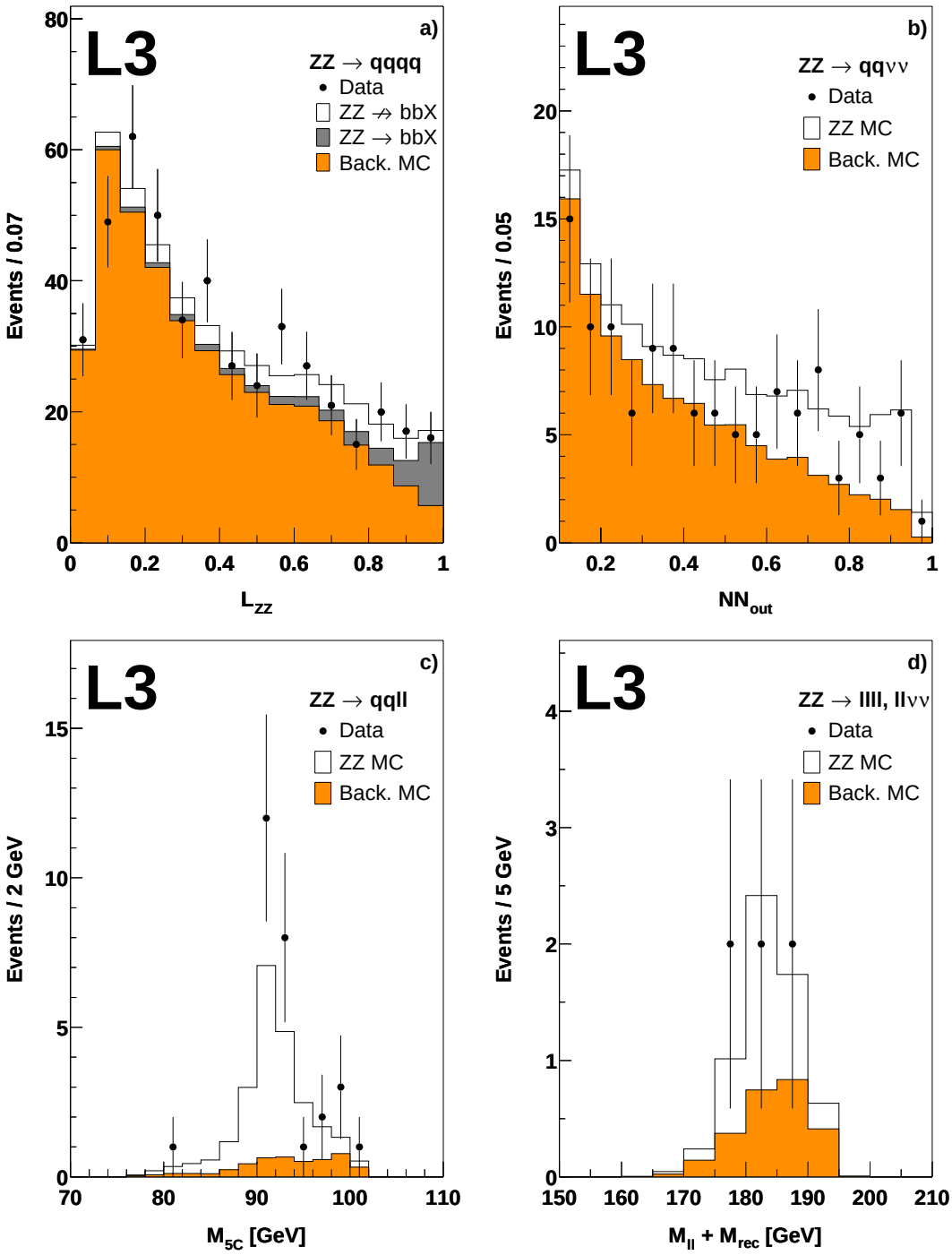

Figure 2: Distribution of the final variables used for the measurement of the cross-section for the a) $q\bar{q}q'\bar{q}'$ b) $q\bar{q}\nu\bar{\nu}$ and c) $q\bar{q}\ell^+\ell^-$ final states. The sum of the $\ell^+\ell^-\nu\bar{\nu}$ and $\ell^+\ell^-\ell'^+\ell'^-$ final states is given in d). The signal and background Monte Carlo distributions are normalised to the expected cross sections.

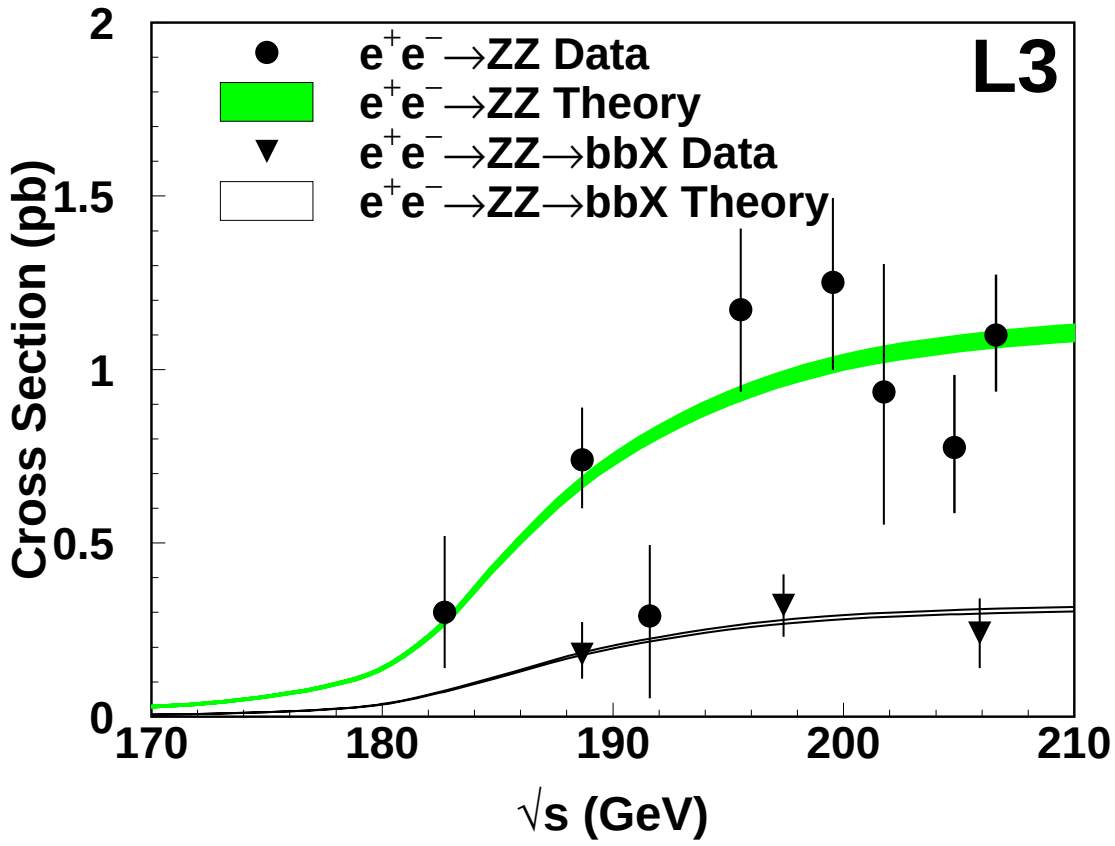

Figure 3: Measurements and predictions for the $e^+e^- \rightarrow ZZ$ and $e^+e^- \rightarrow ZZ \rightarrow b\bar{b}X$ cross sections as a function of $\sqrt{s}$. An uncertainty of 2% is assigned to the predictions.

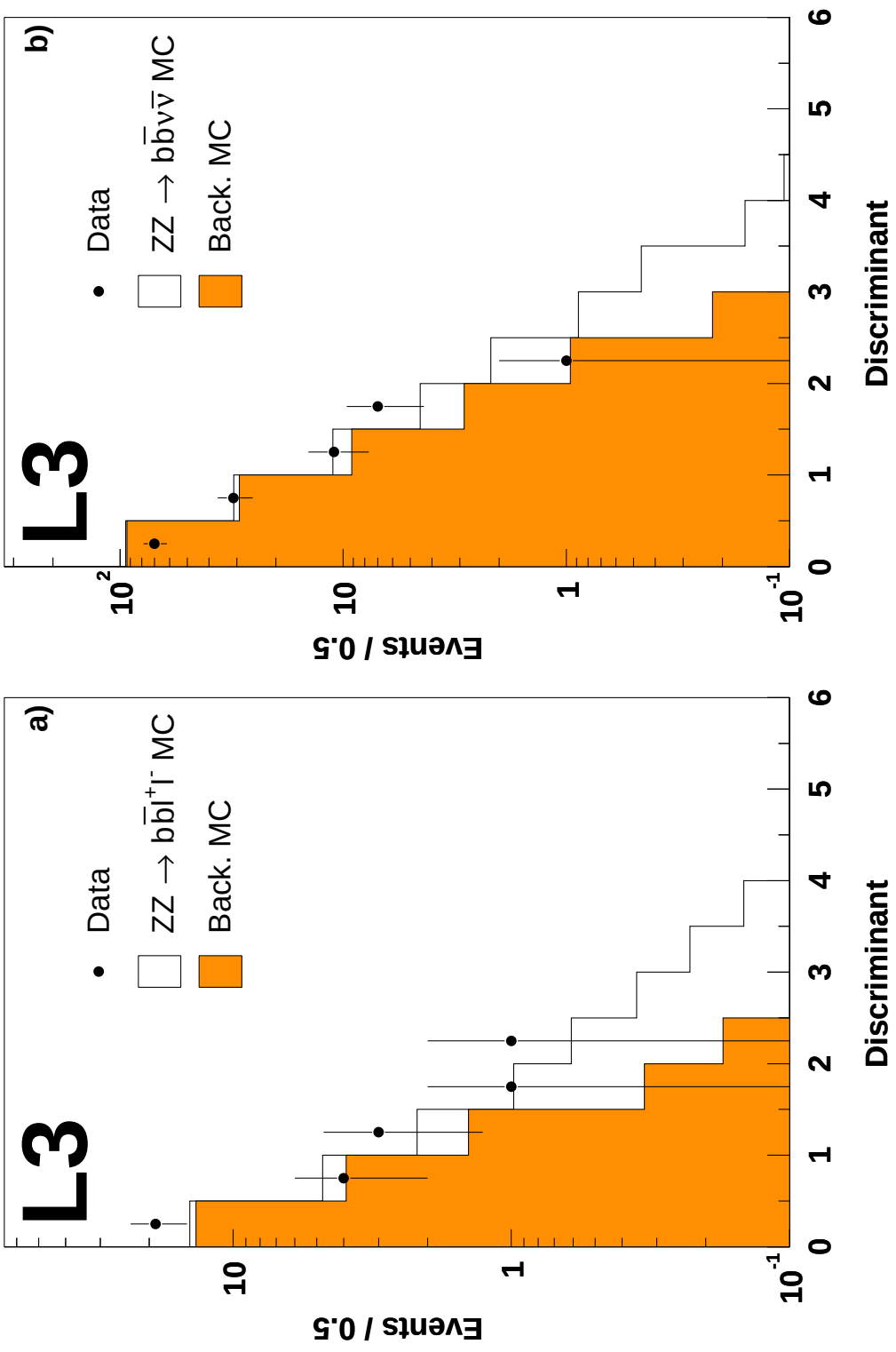

Figure 4: Discriminant variables in data and Monte Carlo for a) the $b\bar{b}\ell^+\ell^-$ and b) the $b\bar{b}\nu\bar{\nu}$ selections. The signal and background Monte Carlo distributions are normalised to the expected cross sections.

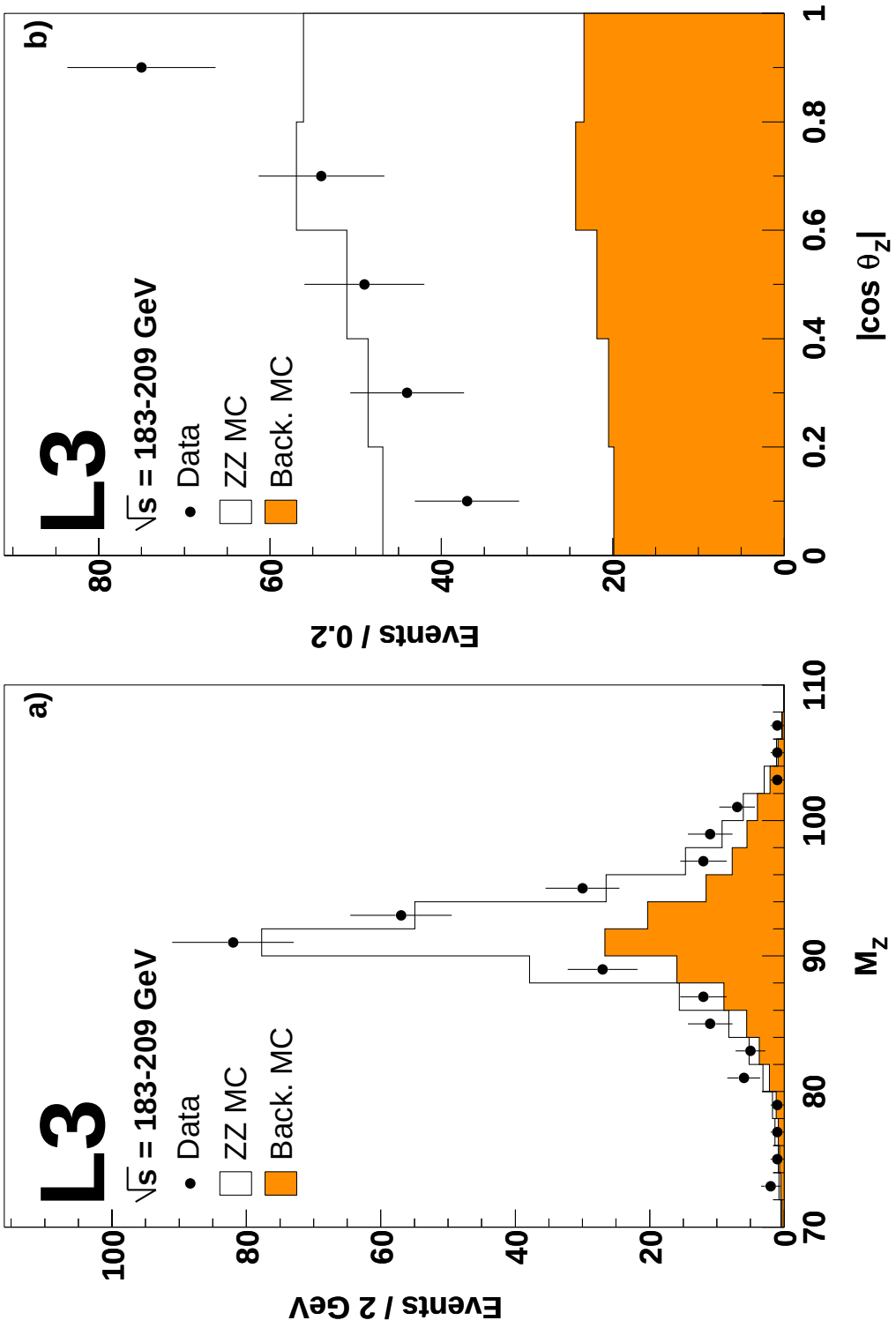

Figure 5: Distributions in data and Monte Carlo at all LEP centre-of-mass energies above the Z pair production threshold of a) the reconstructed mass M and b) the absolute value of the cosine of the production angle θ_Z. Cuts on the $q\bar{q}q'\bar{q}'$ final discriminant and on the $q\bar{q}\nu\bar{\nu}$ neural network output are applied. The signal and background Monte Carlo distributions are normalised to the expected cross sections.

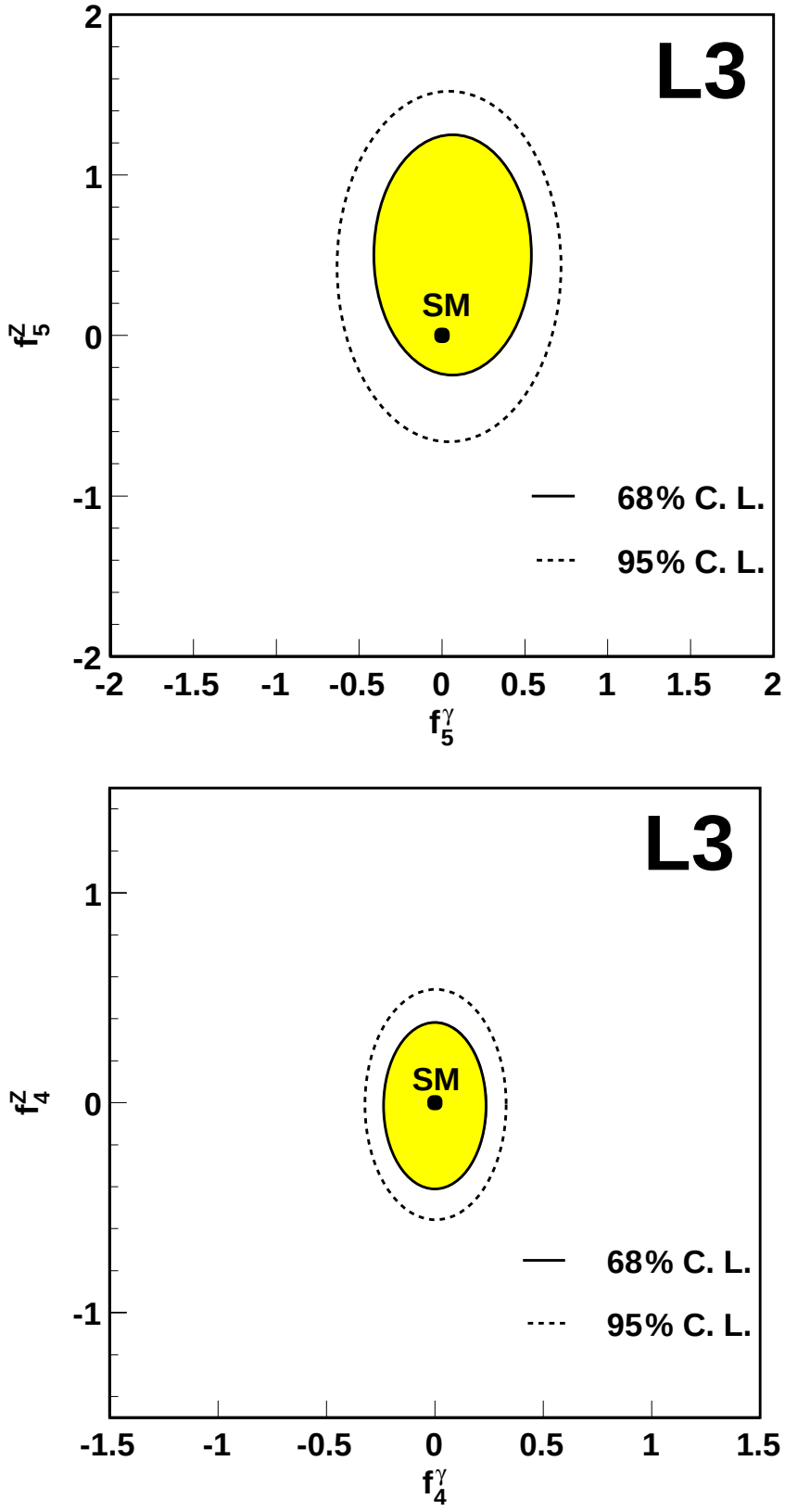

Figure 6: Results of a simultaneous fit to anomalous coupling parameters with the same CP eigenvalue. The Standard Model (SM) expectations are also indicated.